Reduced FOXO1 accelerates skin wound healing and attenuates scarring

Ryoichi Mori[1]*, Katsuya Tanaka[1, 2], Maiko de Kerckhove[1, 4], Momoko Okamoto[1], Kazuya Kashiyama[2], Katsumi Tanaka[2], Sang Eun Kim[1], Takuya Kawata[1], Toshimitsu Komatsu[1], Seongjoon Park[1], Kazuya Ikematsu[3], Akiyoshi Hirano[2], Paul Martin[5] and Isao Shimokawa[1]

[1]Departments of Pathology, [2]Plastic and Reconstructive Surgery, and [3]Forensic Pathology and Science, School of Medicine, Graduate School of Biomedical Sciences, Nagasaki University, 1-12-4 Sakamoto, Nagasaki 852-8523, Japan

[4]Center for Medical Education and Research, Nagasaki Municipal Hospital, 6-39 Shinchi-machi, Nagasaki 850-8555, Japan

[5]Schools of Biochemistry and Physiology & Pharmacology, Faculty of Medical and Veterinary Sciences, University of Bristol, University Walk, Bristol BS8 1TD, UK

*To whom correspondence should be addressed:

Ryoichi Mori, Ph.D.

Department of Pathology, Graduate School of Biomedical Sciences, Nagasaki University, 1-12-4 Sakamoto, Nagasaki 852-8523, Japan

Tel: +81-95-819-7051

Fax: +81-95-819-7052

E-mail: ryoichi@nagasaki-u.ac.jp

Short title: Foxo1 in skin wound healing and scarring

Grants: This work was supported in part by the Ministry of Education, Culture, Sports, Science and Technology of Japan (Grants-in-Aid for Young Scientists [A] 21689049 and 24689069, Challenging Exploratory Research 23650484 and 25560055 to R.M.), Takeda Science Foundation (R. M.), Uehara Memorial Foundation (R. M.), and Nakatomi Foundation (R. M.), The Wellcome Trust (Senior Investigator Award 097791MA P. M.), and The Royal Society (International Joint Project, R. M. and P. M.).

Number of text pages, 49; Figures, 6; Tables; 3

Summary (219 words)

The FOXO family has been extensively investigated in aging and metabolism, but its role in tissue-repair processes remains largely unknown. In the present study, we aimed to clarify the molecular aspect of the FOXO family in skin wound healing. We demonstrated that Foxo1 and Foxo3a were both upregulated during murine skin wound healing. Partial full body knockout of *Foxo1* in *Foxo1*$^{+/-}$ mice led to accelerated skin wound healing with enhanced keratinocyte migration, reduced granulation tissue formation, and collagen density, accompanied by an attenuated inflammatory response, but we observed no wound phenotype in *Foxo3a*$^{-/-}$ mice. Fibroblast growth factor2, adiponectin, and notch1 genes were significantly increased at wound sites in *Foxo1*$^{+/-}$ mice, along with markedly altered ERK1/2 and AKT phosphorylation. Similarly, transient knockdown of Foxo1 at the wound site by local delivery of antisense oligodeoxynucleotides enhanced skin wound healing. The link between FOXO1 and scarring extends to clinical patients, in particular keloid scars where we see FOXO1 expression markedly increased in fibroblasts and inflammatory cells within the otherwise normal dermis in the immediate vicinity of the keloid by comparison to the center of the mature keloid, indicating that FOXO1 is associated with the overgrowth of this fibrotic response into adjacent normal skin. Overall, our data indicate that molecular targeting of FOXO1 may improve the quality of healing and reduce pathological scarring.

Introduction

The skin is our surface organ and, as such plays a major role in protecting us against all extrinsic traumatic factors (i.e. microbes, ultraviolet radiation, heat, and chemicals). Damage to the skin immediately triggers tissue repair mechanisms alongside a robust inflammatory response for host defense.[1] Skin wound healing is generally considered to consist of 3 phases: inflammation, proliferation/migration, and maturation. During an acute wound inflammatory response, large numbers of neutrophils rapidly migrate into damaged tissues to protect against microbes, followed by macrophages that contribute to formation of an associated granulation tissue, including the wound angiogenic response; unfortunately, this wound inflammatory response also contributes to the final fibrotic outcome of adult tissue repair.[2] In parallel with connective tissue repair, epithelial cells migrate over the newly forming granulation tissue to cover the wound site in a process known as re-epithelialisation.[3] Finally, the wound tissues are partially remodeled, including some removal of excess extracellular matrix at the scar site by proteolytic degradation.[4]

Tissue repair speed and quality is dependent on aging, and metabolic status at a whole-body level, in addition to local immunity and cellular responses at the wound site.[5, 6] The skin is one of the clearest indicators of aging, and skin healing is highly associated with the aging process. Skin repair occurs perfectly, without scarring, until fairly late in gestation (embryonic 14 days (d) in the mouse and the end of the second trimester in humans).[7] By contrast the elderly are known to exhibit impaired healing. To date, several studies have therefore focused on the molecular mechanisms linking tissue

repair and skin biology with age- and/or metabolic-related genes.[8-12] A worldwide increase in patients with delayed skin wound healing due to an abnormal healing process is linked with aging, diabetes, malnutrition, chemotherapy, and hereditary diseases.

The mammalian forkhead box O (FOXO) is a family of transcription factors consisting of FOXO1, FOXO3A, FOXO4, and FOXO6. These proteins remain transcriptionally active in the nucleus in the absence of environmental and growth factors.[13] Modification of FOXO leads to its translocation to the cytoplasm and/or its degradation, resulting in the suppression of transcriptional activity. *Foxo1* deficiency (*Foxo1*$^{-/-}$) in embryonic mice has been shown to be lethal, causing abnormal vascular development.[14, 15] We have previously reported that FOXO1 plays a key role in aging and in caloric restriction and exhibits anti-neoplastic characteristics.[16] Several lines of evidence suggest that FOXO proteins may play several key roles during tissue repair. Sarcopenia is an age-associated degenerative condition resulting in the loss of skeletal muscle mass and muscle tissue repair.[17] Activation of the FOXO family is implicated in skeletal muscle regeneration.[18] In human skin wounds, *Foxo1* and *Foxo4* are overly expressed in the transcription factor binding sites of promoters from many differentially expressed genes in the epidermis.[19] Moreover, in diabetic mice, impaired skin wound healing is associated with enhanced activation of FOXO1.[20] Other studies have recently reported that re-epithelialization during scalp wound healing is impaired in keratinocyte-specific *Foxo1*$^{-/-}$ mice.[21] However, the full involvement of FOXO family members and their mechanism of action in all cell lineages involved in skin wound

healing and scarring *in vivo* remain largely unknown.

In the present study, we aimed to investigate the molecular functions for FOXO family gene members in skin wound healing, and their potential application in a clinical setting. We find that heterozygous Foxo1-deficient (*Foxo1*$^{+/-}$) mice exhibit accelerated skin wound healing, decreased scarring, and enhanced keratinocyte migration. Acute knockdown of the FOXO1 protein at wound sites (using Foxo1 antisense oligodeoxynucleotides [AS ODN]) improved the quality of healing. And we suggest that FOXO1 may be implicated in the development of human keloids, since the altered expression of FOXO1 during this process is race-dependent. Our findings suggest that modulating expression of FOXO1 may regulate wound healing and scar formation and thus are potential therapeutic targets for improving wound healing in the clinic.

Materials and methods

Wound model

All experiments were conducted according to the Ethics Review Committee for Animal Experimentation at Nagasaki University (No. 1108010940-7 and 1311121101). The generation of *Foxo1*$^{+/-}$ and *Foxo3a*$^{-/-}$ mice has been described previously.[16, 22] The wound model was performed as previously described[23]. In brief, four full-thickness excisional (4-mm biopsy punch; Kai Industries, Tokyo, Japan) wounds or 2 full-thickness incisional wounds (1-cm) in the dorsal skin (after shaving under anesthesia) were performed in mice (7–12 wks old). Wounds were then harvested using a 6-mm biopsy punch (Kai Industries) and recorded using a digital camera. Areas were calculated using PhotoshopCS4 (Adobe systems, San Jose, CA).

Human samples

Human keloid tissue samples were harvested from Japanese and African American patients at the time of surgery, and diagnosis was confirmed by routine pathological examination (Supplemental Information Table S1). Normal skin tissue samples were harvested from the immediate vicinity of the keloid site. All experiments were conducted with the approval of the ethics committee of Nagasaki University Hospital (No.09062523-2), and in accordance with the Declaration of Helsinki principles. Written informed consent was obtained from each individual.

Histology

Tissue was fixed in 4% PFA for paraffin embedding. Sections (6 μm thick) were used for various staining techniques: H&E, Masson's Trichrome, Picrosirius red staining, and immunohistochemistry (IHC) for FOXO1, neutrophils, F4/80, proliferating cell nuclear antigen (PCNA), and phospho–extracellular signal-regulated kinase (pERK). Observations were made via microscopy (polarized light, epifluorescence, or confocal [C2+ system; Nikon Corporation, Tokyo, Japan]). NIS-Elements C or AR software (Nikon Corporation) was used for data analysis. Immunostaining procedures and antibody information are listed in Table 1.

Analysis of epithelial tongue and area of granulation tissue

Measurement of epithelial tongue and area of granulation tissue were performed as previously described.[23] In brief, the epithelial tongue on H&E-stained wound sections and areas of granulation tissue on Masson's Trichrome staining sections were measured using NIS-Elements AR software.

Analysis of angiogenesis

Wounded skin was fixed in 4% PFA for 16 hours (h), then exposed to 10%, 20%, and 30% sucrose (each percentage for 16 h), and frozen in OCT compound. Sections (50 μm thick) were permeabilized with histology blocking reagent (Blocking One Histo, Nacalai Tesque, Kyoto, Japan) and 0.3% Triton X-100 for 2 h. IHC for CD31, including antibody information are listed in Table 1. Evaluation of 3-dimensional imaging for blood vessels and vascular density were obtained by confocal microscopy,

NIS-Elements C software, and IMARIS software (BITPLANE, Zurich, Switzerland).

Transmission electron microscopy (TEM) and morphological analysis of collagen

TEM and morphological analysis of collagen were performed as previously described.[23, 24]

Measurement of macrophages and FOXO1-positive cells at human intact skin and keloid sites

F4/80-positive cells (indicative of macrophages) and FOXO1-positive cells in the wound bed (defined as the area surrounded by unwounded skin, fascia, regenerated epidermis, and eschar), keloids, or intact skin were counted from 3 random fields (0.14 mm^2).

RNA isolation and quantitative polymerase chain reaction (qPCR)

RNA isolation and qPCR were performed as previously described.[24] The gene-specific primers and probes for qPCR analysis were obtained from TaqMan gene expression assays (Applied Biosystems, Foster City, CA) and gene-specific primer sets (Takara Bio, Shiga, Japan).

Extraction of nuclear protein and measurement of FOXO1 activity

Nuclear proteins were extracted by the Nuclear Extract kit (Active Motif Japan, Tokyo, Japan), according to the manufacturer's instructions. Harvested skin wound sites were homogenized using TissueLyzer II (Qiagen, Hilden, Germany).

FOXO activity was measured with the TransAM FKHR (FOXO1/4) (Active motif Japan) according to the manufacturer's instructions. FOXO1 consensus oligonucleotide-treated extracts were used as the negative control. Absorbance was read by the spectrophotometer (model; LS-PLATEmanager 2004, Wako Pure Chemical Industries, Osaka, Japan). The degree of FOXO1 binding activity was calculated as follows: FOXO1 binding activity (arbitrary units) = optical density/μg of nuclear protein.

Total protein extraction and western immunoblotting

Harvested skin wound sites were homogenized using TissueLyzer II (Qiagen) and were added to T-PER Reagent (Thermo Fisher Scientific, Waltham, MA) consisting of proteinase and dephosphorylation inhibitor (Thermo Fisher Scientific). Supernatant debris was eliminated using Ultrafree-MC 0.45 μm filter (Millipore, Bedford, MA). Filtered protein samples were separated on a 4–12% NuPAGE Novex Bis-Tris gel (Life Technology, Carlsbad, CA), transferred to PVDF, and blotted according to standard protocols (antibody details are listed in Table 1). Protein bands were visualized by chemiluminescence (Thermo Fisher Scientific), and band intensity was calculated using Image J 1.47a software (National Institutes of Health).

Cell culture, Foxo1 siRNA treatment, wound scratch assay, and measurement of pERK activity

Mouse primary keratinocytes (PKs) (Cell Lines Service, Eppelheim, Germany) were

transfected with 100 nM Stealth RNAi Negative Control Medium GC Duplex #2 or Stealth Foxo1 siRNA (Life Technologies, Carlsbad, CA) using the Neon Transfection System (1400 V, 20 ms, 2 pulses) (Life Technologies). The wound scratched assay was performed as previously described.[25] Recombinant mouse fibroblast growth factor 2 (FGF2) (100 ng/mL) (Cell Signaling Technology, Danvers, MA) was used. The intensity of pERK fluorescence was measured by NIS-Elements AR software (Nikon Corporation)

Lipopolysaccharide (LPS) challenge

LPS (from E.coli serotype O55, phenol extraction, was obtained from Wako Pure Chemical Industries) was reconstituted in saline. Mice (8-12 wks, body weight 30 g) were intraperitoneally injected with 1.0 mg of LPS, and their survival was monitored.

ELISA

Extracted proteins were measured by the myeloperoxidase (MPO) mouse ELISA kit (abcam, Cambridge, UK), according to the manufacturer's instructions.

Microarray analysis

Cyanine3-labeled complementary RNA (Cy3-cRNA) was generated from 200 ng of total RNA using the Low input quick amp labeling kit, one color (Agilent Technologies, Santa Clara, CA), and was purified by the RNeasy mini kit (Qiagen), according to the manufacturer's instructions. Fragmented Cy3-cRNA (600 ng) was hybridized to

SurePrint G3 mouse GE microarray, 8 × 60 K (Agilent Technologies) at 65°C for 17 h. The microarray was then washed, and scanned using the Agilent DNA microarray scanner.

Analysis of microarray data was performed using Ingenuity iReport (Ingenuity System, Redwood City, CA). Probeset intensities were summarized and normalized using Robust Multi-Array Average. Significant differential expression was determined by a moderated t-test (Limma) using a p value cutoff of 0.05 and a fold-change cutoff of 1.5. All raw data are available in the GEO database (GSE48473, http://www.ncbi.nlm.nih.gov/geo/query/acc.cgi?acc=GSE48473).

Screening AS ODNs candidates for knockdown studies

AS ODNs and the *in vitro* AS ODN cleavage experiments were both designed as previously described.[23] BLAST searches for AS ODNs sequences (Table 2) were conducted to exclude any sequences that were nonspecific for Foxo1 mRNA (GenBank; NM_019739). Foxo1 mRNA was transcribed from the Riken FANTOM FLS Clone (Clone ID: E430027H20; DNAFORM, Kanagawa, Japan)

For *in vivo* experiments involving ODN delivery, ODNs (1 or 10 μM in 50 μL 30% Pluronic F-127 gel [Sigma-Aldrich, St. Louis, MO], which acts as a slow release vehicle[23]) were topically applied immediately after wounding (50 μL; 1 or 10 μM of ODNs).

Statistical analysis

All data are expressed as the mean ± SEM. Statistical significance was assessed by analysis of variance, followed by: (1) Tukey's post hoc test for multiple comparisons; (2) Dunnett's post hoc test for comparisons of all columns vs. control; or (3) paired or unpaired Student's t-test. Survival curve were analyzed using Kaplan-Meier survival analysis and were compared with the log-rank test. Statistical analysis was performed using GraphPad Prism software (GraphPad Software, La Jolla, CA). Significance was reached at values of $p<0.05$.

Results

Skin wound healing was accelerated in *Foxo1*$^{+/-}$ mice

We investigated the expression of Foxo in wild type (WT) mice after dorsal aseptic skin wounding by qPCR. Gene expression of Foxo1 was significantly increased 3 and 7 d after injury and Foxo3a, 7 d after injury by comparison with unwounded skin (Figure 1A). Gene expression of Foxo4 was markedly low, and Foxo6 was not significantly induced. These results indicated that Foxo1 and Foxo3a genes are the Foxo family members predominantly expressed during the skin repair process.

We then explored the role of FOXO1 and FOXO3A in skin wound healing in *Foxo1*$^{+/-}$ and *Foxo3a*$^{-/-}$ male mice, respectively. *Foxo1*$^{+/-}$ male mice are viable despite expressing less than 50% of both FOXO1 in intact skin (data not shown), and Foxo1 mRNA in liver, spleen, muscle, adipose tissue, and hippocampus.[16] After 3 d of injury, *Foxo1*$^{+/-}$ mice exhibited a significantly smaller wound area (57 ± 3.2%) by comparison to time-matched WT mice (72 ± 4.0%) (Figure 1, B and C). By contrast, wound closure

in *Foxo3a*$^{-/-}$ mice was not altered compared with WT mice (data not shown). These results prompted us to further analyze the function of FOXO1 in skin wound healing.

To determine which cells express FOXO1 protein during skin wound healing, we performed IHC analysis. By only 1 d post injury, FOXO1 was markedly present in the leading edge and basal layer of keratinocytes, and hair follicles, and in recruited neutrophils (Figure 1D and Supplementary Figure S1). Seven d after injury, FOXO1 was present in macrophages, fibroblasts, and endothelial cells at the wound site (Figure 1, E and F). Histological analysis allowed us to quantify both the extent of re-epithelialization and the area of granulation tissue at various time points during repair. The length of epithelial wound tongues in *Foxo1*$^{+/-}$ mice 3 d after injury was markedly higher (813 ± 94 μm) than for WT mice (513 ± 52 μm) (Figure 1, G and H). IHC for the proliferation marker, PCNA, showed that the percentage of proliferating cells in the epithelial tongue of *Foxo1*$^{+/-}$ mice 3 d after injury was markedly increased compared with WT mice (55% versus 40%). Masson's Trichrome staining of sections of excisional wounds revealed that the area of granulation tissue in the mid-wound region of *Foxo1*$^{+/-}$ mice was significantly reduced (0.15 ± 0.014 mm^2) compared with WT mice (0.26 ± 0.021 mm^2) (Figure 1, I and J).

Since angiogenesis is crucial for granulation tissue formation, and FOXO1 is known to be involved in vasculogenesis in embryonic and fetal development [14] we investigated vessel outgrowth during the repair process in *Foxo1*$^{+/-}$ versus WT mice. The 3-dimensional blood vessel network of the wound was reconstructed via confocal microscopy of sections stained for for PECAM/CD31 which is a marker for endothelial

cells.[26] These studies revealed no difference in the vessel network in intact skin of *Foxo1*$^{+/-}$ and WT mice (0.033 ± 0.0024 μm^3/μm^3 and 0.026 ± 0.0057 μm^3/μm^3, respectively) and the same was true at both 7 and 14 d wound sites (Supplemental Figure S2).

Our analyses suggest that attenuated expression of FOXO1 protein leads to accelerated repair and improved quality of skin wound healing, owing to enhanced migration of keratinocytes in the early stage of wound healing, followed by decreased area of granulation tissue formation, but this is not due to differences in wound angiogenesis.

The inflammatory response was attenuated at wound sites of *Foxo1*$^{+/-}$ mice

Several leukocyte lineages infiltrate wound sites at various time points during the skin repair process.[2] Our IHC staining showed that wound-infiltrated neutrophils and macrophages expressed FOXO1 protein (Figure 1, D and E). Neutrophils, revealed either by neutrophil IHC or measurement of MPO were reduced in *Foxo1*$^{+/-}$ wounds versus WT controls (Figure 2, A and B). F4/80 IHC for macrophages[27] confirms a similar reduction (by 40%) in macrophage numbers at wound sites of *Foxo1*$^{+/-}$ mice (Figure 2, C and D).

Since NF-κB plays a pivotal role in the inflammatory response[28] we performed western immunoblot analysis and showed that phosphorylation levels of NF-κB p65 (Ser536) at wound sites of *Foxo1*$^{+/-}$ mice 3 d after injury were markedly reduced (by 38%) compared with WT mice (Figure 2, E and F). In addition, we found that *Foxo1*$^{+/-}$

mice exhibited significant resistance to high dose LPS-induced endotoxin shock that leads to activation of NF-κB signaling via TLR4 *in vivo* (Supplemental Figure S3).[29] Collectively, these data suggest that FOXO1 may regulate inflammatory cell recruitment to wound sites, and the reduced FOXO1 in *Foxo1*$^{+/-}$ mice dampens down this inflammatory response.

Expression and phosphorylation of the FOXO family at wound sites

Our findings provide clear evidence that *Foxo1*$^{+/-}$ mice exhibit accelerated skin wound healing and enhanced re-epithelialization at the early stage of skin wound healing and a diminished inflammatory response. We next performed a comprehensive gene expression profile at wound sites of *Foxo1*$^{+/-}$ and WT mice, after first confirming reduced FOXO1 DNA binding activity. ELISA studies indicate reduced binding of FOXO1 in cells from wound sites of *Foxo1*$^{+/-}$ mice 3 and 7 d after injury (66 ± 13% and 56 ± 15%, respectively) compared with WT mice (Figure 3A). Similar results were found for both gene (Table 3) and protein (Figure 3B) expression of FOXO1.

In human fibroblasts, FOXO1 and FOXO3A have been shown to impact on Foxo1 gene expression,[30] and so we examined the protein expression and phosphorylation levels of FOXO1, FOXO3A, and FOXO4 at wound sites 3 d after injury *Foxo1*$^{+/-}$ mice (Figure 3B). We find that FOXO1 protein expression and its phosphorylation (pFOXO1 [Thr24]) level at wound sites were markedly decreased in *Foxo1*$^{+/-}$ mice, but expression of FOXO3A, pFOXO3A (Ser318/321), and FOXO4 were not altered in either group. These results, and the pattern of expression of Foxo family genes during skin repair

(Figure 1A) indicates that FOXOs at the wound site are predominantly regulated by pFOXO1 (Thr24) and pFOXO3A (Ser318/321) in the early stage of skin wound healing.

Activation of ERK1/2 was enhanced in wound sites of *Foxo1*$^{+/-}$ mice

To determine the molecular mechanisms underlying enhanced skin wound healing when FOXO1 protein expression was reduced, we performed microarray analysis on 3 d skin wound samples from *Foxo1*$^{+/-}$ versus WT mice. Using a fold-change cutoff of 1.5 (with a p-value cutoff of 0.05), we identify 387 and 269 genes differentially regulated genes (DRGs) that are up- and down-regulated in *Foxo1*$^{+/-}$ mice, respectively (Supplementary Table S2). We next screened for those molecules/pathways that might be most likely to be promoting healing in *Foxo1*$^{+/-}$ mice by analyzing the molecular interactions between DRGs, such as gene expression, activation, post-translational modification, and physical interactions (Supplementary Table S3). Previous *in vivo* studies have revealed skin wound healing-related genes: fibroblast growth factor2 (*Fgf2*),[31-33] Adiponectin (*Adipoq*),[8, 9] and *Notch1*.[34] Our results showed that Fgf2, Adipoq, and Notch1 were significantly ($p < 0.05$) increased 1.65-fold, 1.82-fold, and 1.94-fold, respectively in 3 d wound sites of *Foxo1*$^{+/-}$ mice (Table 3).

Two key signaling pathways may contribute to the FOXO1 phenotype we observe. The ERK1/2 signaling pathway is involved in cell migration and proliferation,[25] and the AKT signaling pathway is associated with skin wound healing functions upstream of FOXO1.[35] The ERK1/2 and AKT pathways are activated by FGF2 and ADIPOQ,

contributing to epithelial and fibroblast cell proliferation.[8, 36] Therefore, we investigated whether activation of ERK and AKT pathways in wound sites of *Foxo1*$^{+/-}$ mice were altered. The phosphorylation levels of ERK1/2 (Thr202/Tyr204) in wound sites of *Foxo1*$^{+/-}$ mice 3 d after injury was markedly increased compared with WT (1.5 ± 0.13 and 1.0 ± 0.11, respectively) (Figure 3C). In contrast, the phosphorylation levels of AKT (Ser473) in wound sites of *Foxo1*$^{+/-}$ mice 7 d after injury was markedly decreased compared with WT (0.56 ± 0.054 and 1.0 ± 0.20, respectively) (Figure 3D).

Our microarray analysis showed that several cell migration- and proliferation-related signals were significantly up-regulated, including myosin heavy chain 10 (Myh10) (1.64-fold). MYH10 generates non-muscle Myosin IIb isoform,[37] which is downstream of the ERK1/2 pathway.[38] Myosin IIb is expressed in both epidermis and wound fibroblasts,[39] and Myh10 is markedly induced at wound sites in *Foxo1*$^{+/-}$ mice (Table 3) in the current study. We also see that protein levels of the Myosin IIb isoform are markedly increased in wound sites of *Foxo1*$^{+/-}$ mice compared with WT (1.5 ± 0.21 and 1.0 ± 0.067, respectively) (Figure 3, C and D). Collectively, these results suggest that expression of Myosin IIb may be enhanced via the ERK pathway at early stage of wound repair in *Foxo1*$^{+/-}$ mice.

We next tested whether FOXO1 was involved in wound FGF2 signaling, which contributes to the enhancement of cell proliferation and migration in PKs. The *in vitro* wound scratch assay demonstrated that wound closure in Foxo1 siRNA-treated PKs was not altered compared with control PKs (1.23 ± 0.15 and 1.0 ± 0.04, respectively). Interestingly, the migration of mFGF2-treated Foxo1 siRNA-treated PKs was

significantly enhanced from the wound edge to the center of the wound (Figure 3, E and F). ICC was then used to investigate the localization of pERK. In PKs exposed to mFGF2-treated Foxo1 siRNA, pERK activation was mainly observed at the wound edge rather than away from the wound site 24 h after scratching. This response was significantly higher compared with control wounds (4.95 ± 0. 63 and 2.82 ± 0.41, respectively) (Figure 3, G and H). Taken together, these findings indicate that FOXO1 may play a role in re-epithelialization and migration of keratinocytes at wound sites via the ERK and FGF2 pathway.

Collagen organization was altered at wound sites of *Foxo1*$^{+/-}$ mice

Scarring is the final consequence of the wound healing process, and is a measure of wound healing quality.[1] To investigate whether altered FOXO1 expression influences the development of scarring at wound sites, we monitored scarring 21 d after making 1-cm incisional wounds to *Foxo1*$^{+/-}$ and WT mice (Figure 4A). Picrosirius red staining showed type I collagen (red and yellow) and type III collagen (green) bundle organization[40] to be markedly reduced in *Foxo1*$^{+/-}$ mice 21 d after injury (Figure 4B).

To further analyze development of scar, we performed TEM to reveal gross collagen bundling patterns, individual collagen fibril diameter, and the density of fibrils at wound site. Morphology of collagen within intact skin of *Foxo1*$^{+/-}$ and WT mice was indistinguishable (Supplemental Figure S4). Interestingly, the fibril diameter at the mid-region wound sites of *Foxo1*$^{+/-}$ mice were markedly ($p < 0.001$) reduced (61.5 ± 0.49 nm) compared with WT mice (63.3 ± 0.46 nm) (Figure 4, C and D). Furthermore,

intra collagen bundle spaces at wound sites of *Foxo1*$^{+/-}$ mice were significantly ($p < 0.05$) increased (0.62 ± 0.094 $\mu m^2/\mu m^2$) compared with WT mice (0.38 ± 0.023 $\mu m^2/\mu m^2$) (Figure 4E), more closely resembling that of unwounded skin. Gene expression of type I collagen α1 (Col1α1), was significantly decreased at wound sites of *Foxo1*$^{+/-}$ mice 7 d after injury compared with WT mice (0.58 ± 0.073 and 0.82 ± 0.063, respectively) (Figure 4F). We suggest that these differences of collagen assembly at wound sites play a key role in reducing scar formation during the maturation phase of healing in *Foxo1*$^{+/-}$ mice.

Acute knock down of FOXO1 using AS ODNs improved skin wound healing

Our *Foxo1*$^{+/-}$ mouse data provides experimental evidence that attenuation of FOXO1 expression may improve skin wound healing. To further address our hypothesis and test whether reducing levels of this transcription factor during the repair process is a potential therapeutic strategy for improving healing, we designed and optimized Foxo1 specific AS ODNs *in vitro* (Figure 5A). We applied Foxo1 AS ODN (1717) (10 μM in 30% Pluronic gel for 6 h at the wound site[23]) versus control ODN, (with sequence predicted to be non-binding to other mRNAs), to 4-mm diameter adult skin wound sites (Figure 5, B and C). Macroscopic analysis indicated that wound closure in Foxo1 AS ODN-treated wound sites 3 d after injury was markedly accelerated (67 ± 2.4%) at early time points during the repair process, compared with the control ODN-treated wound (76 ± 3.0%) (Figure 5, D and E). Next, we made a 1-cm incisional wound in the dorsal skin and analyzed scarring (via TEM) with a 21-d treatment of control ODN or Foxo1

AS ODN at the wound sites. The fibril diameter at the mid-region was not altered (66.6 ± 0.65 nm, n = 1336 from 3 mice) at Foxo1 AS ODN-treated wound sites compared with control ODN-treated wound site (65.1 ± 0.55 nm, n = 1534 from 3 mice). Neither was vacant extracellular space at Foxo1 AS ODN-treated wound sites altered (0.55 ± 0.038 $\mu m^2/\mu m^2$, n = 3) compared with control ODN-treated wound sites (0.44 ± 0.038$\mu m^2/\mu m^2$, n = 3). These results indicated that acute down-regulation of FOXO1 protein at the wound site using Foxo1 AS ODN accelerated skin wound healing, but did not significantly alter scar quality.

Increased FOXO1 is associated with human keloid scars

Because of the altered level of scarring in our whole body *Foxo1*$^{+/-}$ mouse studies, we next chose to investigate whether the expression pattern of FOXO1 was altered in human keloid scars, which are an extreme instance of human skin fibrotic disease, typified by a hypertrophic epidermis, and overgrowth of granulation tissue which expands in a claw-like way to invade adjacent normal skin.[41, 42] IHC showed that FOXO1 was prominently present in suprabasal keratinocytes of the hypertrophic epidermal layer of keloids (Figure 6A), in addition to some fibroblasts and inflammatory cells (Figure 6B). Although FOXO1 in fibroblasts was not strongly expressed at deep keloid tissue sites (Figure 6C), it was notably present in numerous fibroblasts and inflammatory cells in the immediate vicinity of keloid sites of the normal dermal layer (Figure 6, D, E and G). These results suggested that FOXO1 was involved in expanding the growth of keloid into adjacent normal skin sites and might be

driving the production of excessive extracellular matrix protein.

The development of a keloid is known to be associated with age, physiological conditions, and genetic backgrounds. Keloids occurs most frequently in individuals of African American descent.[43] Therefore, we next performed a comparative case report of keloids between African American and Japanese to investigate the expression of FOXO1. Levels of expression of FOXO1 in keratinocytes, fibroblasts, and inflammatory cells in all keloid sites was markedly higher in African Americans compared with Japanese (Figure 6, F and H). Collectively, these results indicate that the development of skin fibrotic diseases may, in part, be regulated by FOXO1 (Figure 6I).

Discussion

In the present study, we report accelerated and improved eventual quality of skin wound healing in *Foxo1*$^{+/-}$ mice, due to enhanced re-epithelialization and a reduced inflammatory response at sites of tissue damage. Foxo1 AS ODN-treated wounds also exhibit improved skin wound healing. Abnormal and diverse expression of FOXO1 is also associated with the development of keloids in human patients. The present data provide a novel molecular insight into the function of FOXO1 in skin wound healing and suggest its potential as an anti-scarring therapeutic target.

Skin wounding initially leads to clot formation and a significant recruitment of neutrophils, which protect the tissue breach by killing microbes and also release proinflammatory cytokines, some of which act to draw in macrophages to the wound also. Thereafter, macrophages infiltrate the wound site and secrete cytokines,

chemokines, and growth factors according to the extent of tissue damage and infection state, thus reflecting the degree of the inflammatory phase.[1] The FOXO family has been previously shown to regulate the homeostasis of the immune system and the inflammatory response.[44] Conditional *Foxo1*$^{-/-}$ mice exhibit an altered phenotype, including T-cell homeostasis and tolerance.[45-47] FOXO1 may play a role during the infection recognition and clearance process [48] since it is known that the bacterial product N-formylmethionyl-leucyl-phenylalanine triggers neutrophils to upregulate myeloid leukemia cell differentiation protein MCL1, which can form a complex with FOXO1. Moreover, Chip-sequencing analysis using next generation sequencing has revealed that FOXO1 significantly enhances TLR4 signaling in macrophages.[49] Activation of NF-κB affects the AKT-FOXO1 signaling pathway.[50] In the present study, the infiltration of neutrophils and macrophages into wound sites and the phosphorylation of NF-κB and AKT were attenuated in *Foxo1*$^{+/-}$ mice. Overall, the FOXO1-mediated inflammatory response may link in to leukocyte recruitment and activation in the skin wound healing process.

Re-epithelialization, involving keratinocyte migration and proliferation, commences soon after skin damage and is regulated by various factors including keratinocyte growth factor and others released by infiltrating inflammatory cells, and fibroblasts.[2, 3] Previous studies suggest that the effect of FOXO1 in guiding cell migration/proliferation may be cell-type specific. For example, knockdown of Foxo1 in PDGF-treated fibroblasts has been shown to enhance proliferation, indicating that attenuation of the expression of FOXO1 is sufficient for the enhancement of cell

growth.[30] In contrast, keratinocyte specific *Foxo1*$^{-/-}$ in mice impairs scalp wound healing due to reduced expression of Tgfβ1.[21] In our current study, enhancement of re-epithelialization in *Foxo1*$^{+/-}$ mice accelerated skin wound healing, which corresponded with an increase in the expression of Fgf2, Adipoq, Notch1, and Myo10 (Table 3), and each of these, in turn, is known to play key roles in various aspects of the repair process: FGF2 is crucial for re-epithelialization in skin wound healing,[33] whilst genetic and pharmacological inhibition of Notch1 in mice markedly impairs skin wound healing,[34] and calmodulin-like protein-mediated expression of MYO10 contributes to keratinocyte motility and migration in humans and mice.[51] ADIPOQ promotes keratinocyte proliferation and migration via the ERK pathway *in vivo*.[8, 9] We are currently exploring the mechanism underlying FOXO-mediated regulation of cell proliferation and migration in the presence of FGF2 at wound sites.

As well as enhanced rate of wound repair, we observe reduced scarring in *Foxo1*$^{+/-}$ mice. Scarring appears at the final stage of the skin wound healing process, and the phenotype of scarring is dependent on diverse factors, including inflammation, delayed healing, physiological condition, age, and race.[6, 43, 52] The regulation of collagen expression via FOXO1 may depend on the tissue and cell type, and this may be a consequence of both direct and/or indirect effects. Knockdown of Foxo1 in UV-irradiated human dermal fibroblasts was shown to significantly decrease the expression of Col1α1.[53] In contrast, expression of liver Col1α1 was increased in the bile duct ligation-induced experimental liver fibrosis model of *Foxo1*$^{+/-}$, resulting in liver fibrosis.[54] Collagen organization is controlled by several enzymes and extracellular

matrix proteins,[55] and considerably altered by normal aging.[56, 57] Activation of AKT is one of the main signaling pathways for type I procollagen synthesis.[58] In the present study, expression of Col1α1, collagen density, and AKT phosphorylation were all markedly decreased in wound sites of *Foxo1*$^{+/-}$ mice 7 d after injury. We also found that knockdown of FOXO1 in PKs significantly enhanced the ERK pathway after mFGF2 application. Local administration of FGF2 to the human incisional wound reduces scarring.[59] We speculate that the attenuation of FOXO1 in wound fibroblasts contributes to reduced scarring through the FGF2 pathway. We are presently exploring how FOXO1 regulates scarring at wound sites in the presence of several wound growth factors, including FGF2. Further studies using other models, such as keratinocyte-specific *Foxo1*$^{-/-}$ mice,[21] are required to better elucidate the pathophysiological significance of FOXO1 function in skin fibrosis.

In patients, the most extreme scarring phenotype is that of keloid scarring where scar tissue spills out from the initial site of tissue damage. Our keloid studies showed FOXO1 is highly expressed in fibroblasts and inflammatory cells at the margin of a keloid compared with those fibroblasts in mature keloid sites, and that FOXO1 expression level was altered between African Americans and Japanese. These results indicate that FOXO1 may regulate the expression of collagen, and thus, its expression level may play a key role in scarring and keloids. Current investigations are focusing on the implications of FOXO1 polymorphisms on fibrotic diseases. Disequilibrium of FOXO1 is believed to affect human longevity,[60, 61] and thus polymorphism of FOXO1 may also affect homeostasis at the cellular and individual level as well. Therefore, a

functional analysis of FOXO1 polymorphisms may further elucidate the differences in keloid morbidity and repair phenotypes by age and race. Determining how the FOXO1 signaling pathway regulates keloid progression for the homeostatic maintenance between proliferation and differentiation will thus be important to explore in future studies.

In conclusion, the age-related gene, FOXO1, plays a central role for tissue repair and remodeling and, may be considered a potential therapeutic target for enhancing tissue repair and remodeling as well as for dampening inflammatory diseases and fibrosis.

Acknowledgments

The authors are grateful to Takashi Suematsu (Department of Electron Microscopy, Nagasaki University) for assistance with the TEM analysis, and Kazutaka Hayashida and Shin-ichi Yokota (Nikon Instech, Japan) for assistance with microscopic and imaging analysis.

Conflict of interest

The authors have no financial conflicts of interest.

References

1. Shaw TJ, Martin P: Wound repair at a glance, J Cell Sci 2009, 122:3209-3213

2. Eming SA, Krieg T, Davidson JM: Inflammation in wound repair: molecular and cellular mechanisms, J Invest Dermatol 2007, 127:514-525

3. Werner S, Krieg T, Smola H: Keratinocyte-fibroblast interactions in wound healing, J Invest Dermatol 2007, 127:998-1008

4. Martins VL, Caley M, O'Toole EA: Matrix metalloproteinases and epidermal wound repair, Cell Tissue Res 2013, 351:255-268

5. Gosain A, DiPietro LA: Aging and wound healing, World J Surg 2004, 28:321-326

6. Guo S, Dipietro LA: Factors affecting wound healing, J Dent Res 2010, 89:219-229

7. Ferguson MW, O'Kane S: Scar-free healing: from embryonic mechanisms to adult therapeutic intervention, Philos Trans R Soc Lond B Biol Sci 2004, 359:839-850

8. Shibata S, Tada Y, Asano Y, Hau CS, Kato T, Saeki H, Yamauchi T, Kubota N, Kadowaki T, Sato S: Adiponectin regulates cutaneous wound healing by promoting keratinocyte proliferation and migration via the ERK signaling pathway, J Immunol 2012, 189:3231-3241

9. Salathia NS, Shi J, Zhang J, Glynne RJ: An in vivo screen of secreted proteins identifies adiponectin as a regulator of murine cutaneous wound healing, J Invest Dermatol 2013, 133:812-821

10. Goren I, Kampfer H, Podda M, Pfeilschifter J, Frank S: Leptin and wound

inflammation in diabetic ob/ob mice: differential regulation of neutrophil and macrophage influx and a potential role for the scab as a sink for inflammatory cells and mediators, Diabetes 2003, 52:2821-2832

11. Squarize CH, Castilho RM, Bugge TH, Gutkind JS: Accelerated wound healing by mTOR activation in genetically defined mouse models, PLoS One 2010, 5:e10643

12. Serravallo M, Jagdeo J, Glick SA, Siegel DM, Brody NI: Sirtuins in dermatology: applications for future research and therapeutics, Arch Dermatol Res 2013, 305:269-282

13. Huang H, Tindall DJ: Dynamic FoxO transcription factors, J Cell Sci 2007, 120:2479-2487

14. Furuyama T, Kitayama K, Shimoda Y, Ogawa M, Sone K, Yoshida-Araki K, Hisatsune H, Nishikawa S, Nakayama K, Ikeda K, Motoyama N, Mori N: Abnormal angiogenesis in Foxo1 (Fkhr)-deficient mice, J Biol Chem 2004, 279:34741-34749

15. Hosaka T, Biggs WH, 3rd, Tieu D, Boyer AD, Varki NM, Cavenee WK, Arden KC: Disruption of forkhead transcription factor (FOXO) family members in mice reveals their functional diversification, Proc Natl Acad Sci U S A 2004, 101:2975-2980

16. Yamaza H, Komatsu T, Wakita S, Kijogi C, Park S, Hayashi H, Chiba T, Mori R, Furuyama T, Mori N, Shimokawa I: FoxO1 is involved in the antineoplastic effect of calorie restriction, Aging Cell 2010, 9:372-382

17. Snijders T, Verdijk LB, van Loon LJ: The impact of sarcopenia and exercise training on skeletal muscle satellite cells, Ageing Res Rev 2009, 8:328-338

18. Lara-Pezzi E, Winn N, Paul A, McCullagh K, Slominsky E, Santini MP, Mourkioti F, Sarathchandra P, Fukushima S, Suzuki K, Rosenthal N: A naturally occurring calcineurin variant inhibits FoxO activity and enhances skeletal muscle regeneration, J Cell Biol 2007, 179:1205-1218

19. Roupe KM, Alberius P, Schmidtchen A, Sorensen OE: Gene expression demonstrates increased resilience toward harmful inflammatory stimuli in the proliferating epidermis of human skin wounds, Exp Dermatol 2010, 19:e329-332

20. Siqueira MF, Li J, Chehab L, Desta T, Chino T, Krothpali N, Behl Y, Alikhani M, Yang J, Braasch C, Graves DT: Impaired wound healing in mouse models of diabetes is mediated by TNF-alpha dysregulation and associated with enhanced activation of forkhead box O1 (FOXO1), Diabetologia 2010, 53:378-388

21. Ponugoti B, Xu F, Zhang C, Tian C, Pacios S, Graves DT: FOXO1 promotes wound healing through the up-regulation of TGF-beta1 and prevention of oxidative stress, J Cell Biol 2013, 203:327-343

22. Miyamoto K, Araki KY, Naka K, Arai F, Takubo K, Yamazaki S, Matsuoka S, Miyamoto T, Ito K, Ohmura M, Chen C, Hosokawa K, Nakauchi H, Nakayama K, Nakayama KI, Harada M, Motoyama N, Suda T, Hirao A: Foxo3a is essential for maintenance of the hematopoietic stem cell pool, Cell Stem Cell 2007, 1:101-112

23. Mori R, Shaw TJ, Martin P: Molecular mechanisms linking wound inflammation and fibrosis: knockdown of osteopontin leads to rapid repair and reduced scarring, J Exp Med 2008, 205:43-51

24. Mori R, Ikematsu K, Kitaguchi T, Kim SE, Okamoto M, Chiba T, Miyawaki

A, Shimokawa I, Tsuboi T: Release of TNF-alpha from macrophages is mediated by small GTPase Rab37, Eur J Immunol 2011, 41:3230-3239

25. Matsubayashi Y, Ebisuya M, Honjoh S, Nishida E: ERK activation propagates in epithelial cell sheets and regulates their migration during wound healing, Curr Biol 2004, 14:731-735

26. Newman PJ: The biology of PECAM-1, J Clin Invest 1997, 99:3-8

27. Austyn JM, Gordon S: F4/80, a monoclonal antibody directed specifically against the mouse macrophage, Eur J Immunol 1981, 11:805-815

28. DiDonato JA, Mercurio F, Karin M: NF-kappaB and the link between inflammation and cancer, Immunol Rev 2012, 246:379-400

29. Kawai T, Akira S: The role of pattern-recognition receptors in innate immunity: update on Toll-like receptors, Nat Immunol 2010, 11:373-384

30. Essaghir A, Dif N, Marbehant CY, Coffer PJ, Demoulin JB: The transcription of FOXO genes is stimulated by FOXO3 and repressed by growth factors, J Biol Chem 2009, 284:10334-10342

31. Meyer M, Muller AK, Yang J, Moik D, Ponzio G, Ornitz DM, Grose R, Werner S: FGF receptors 1 and 2 are key regulators of keratinocyte migration in vitro and in wounded skin, J Cell Sci 2012, 125:5690-5701

32. Miller DL, Ortega S, Bashayan O, Basch R, Basilico C: Compensation by fibroblast growth factor 1 (FGF1) does not account for the mild phenotypic defects observed in FGF2 null mice, Mol Cell Biol 2000, 20:2260-2268

33. Ortega S, Ittmann M, Tsang SH, Ehrlich M, Basilico C: Neuronal defects and

delayed wound healing in mice lacking fibroblast growth factor 2, Proc Natl Acad Sci U S A 1998, 95:5672-5677

34. Chigurupati S, Arumugam TV, Son TG, Lathia JD, Jameel S, Mughal MR, Tang SC, Jo DG, Camandola S, Giunta M, Rakova I, McDonnell N, Miele L, Mattson MP, Poosala S: Involvement of notch signaling in wound healing, PLoS One 2007, 2:e1167

35. Somanath PR, Chen J, Byzova TV: Akt1 is necessary for the vascular maturation and angiogenesis during cutaneous wound healing, Angiogenesis 2008, 11:277-288

36. Chrissouli S, Pratsinis H, Velissariou V, Anastasiou A, Kletsas D: Human amniotic fluid stimulates the proliferation of human fetal and adult skin fibroblasts: the roles of bFGF and PDGF and of the ERK and Akt signaling pathways, Wound Repair Regen 2010, 18:643-654

37. Conti MA, Adelstein RS: Nonmuscle myosin II moves in new directions, J Cell Sci 2008, 121:11-18

38. Kim JH, Wang A, Conti MA, Adelstein RS: Nonmuscle myosin II is required for internalization of the epidermal growth factor receptor and modulation of downstream signaling, J Biol Chem 2012, 287:27345-27358

39. Bond JE, Ho TQ, Selim MA, Hunter CL, Bowers EV, Levinson H: Temporal spatial expression and function of non-muscle myosin II isoforms IIA and IIB in scar remodeling, Lab Invest 2011, 91:499-508

40. Wang T, Feng Y, Sun H, Zhang L, Hao L, Shi C, Wang J, Li R, Ran X, Su Y,

Zou Z: miR-21 regulates skin wound healing by targeting multiple aspects of the healing process, Am J Pathol 2012, 181:1911-1920

41. Hunasgi S, Koneru A, Vanishree M, Shamala R: Keloid: A case report and review of pathophysiology and differences between keloid and hypertrophic scars, J Oral Maxillofac Pathol 2013, 17:116-120

42. Robles DT, Moore E, Draznin M, Berg D: Keloids: pathophysiology and management, Dermatol Online J 2007, 13:9

43. Shih B, Bayat A: Genetics of keloid scarring, Arch Dermatol Res 2010, 302:319-339

44. Peng SL: Foxo in the immune system, Oncogene 2008, 27:2337-2344

45. Gubbels Bupp MR, Edwards B, Guo C, Wei D, Chen G, Wong B, Masteller E, Peng SL: T cells require Foxo1 to populate the peripheral lymphoid organs, Eur J Immunol 2009, 39:2991-2999

46. Ouyang W, Beckett O, Flavell RA, Li MO: An essential role of the Forkhead-box transcription factor Foxo1 in control of T cell homeostasis and tolerance, Immunity 2009, 30:358-371

47. Ouyang W, Liao W, Luo CT, Yin N, Huse M, Kim MV, Peng M, Chan P, Ma Q, Mo Y, Meijer D, Zhao K, Rudensky AY, Atwal G, Zhang MQ, Li MO: Novel Foxo1-dependent transcriptional programs control T(reg) cell function, Nature 2012, 491:554-559

48. Crossley LJ: Neutrophil activation by fMLP regulates FOXO (forkhead) transcription factors by multiple pathways, one of which includes the binding of FOXO

to the survival factor Mcl-1, J Leukoc Biol 2003, 74:583-592

49. Fan W, Morinaga H, Kim JJ, Bae E, Spann NJ, Heinz S, Glass CK, Olefsky JM: FoxO1 regulates Tlr4 inflammatory pathway signalling in macrophages, EMBO J 2010, 29:4223-4236

50. Kim DH, Kim JY, Yu BP, Chung HY: The activation of NF-kappaB through Akt-induced FOXO1 phosphorylation during aging and its modulation by calorie restriction, Biogerontology 2008, 9:33-47

51. Bennett RD, Mauer AS, Pittelkow MR, Strehler EE: Calmodulin-like protein upregulates myosin-10 in human keratinocytes and is regulated during epidermal wound healing in vivo, J Invest Dermatol 2009, 129:765-769

52. Martin P, Leibovich SJ: Inflammatory cells during wound repair: the good, the bad and the ugly, Trends Cell Biol 2005, 15:599-607

53. Tanaka H, Murakami Y, Ishii I, Nakata S: Involvement of a forkhead transcription factor, FOXO1A, in UV-induced changes of collagen metabolism, J Investig Dermatol Symp Proc 2009, 14:60-62

54. Adachi M, Osawa Y, Uchinami H, Kitamura T, Accili D, Brenner DA: The forkhead transcription factor FoxO1 regulates proliferation and transdifferentiation of hepatic stellate cells, Gastroenterology 2007, 132:1434-1446

55. Canty EG, Kadler KE: Procollagen trafficking, processing and fibrillogenesis, J Cell Sci 2005, 118:1341-1353

56. Puschmann S, Rahn CD, Wenck H, Gallinat S, Fischer F: Approach to quantify human dermal skin aging using multiphoton laser scanning microscopy, J

Biomed Opt 2012, 17:036005

57. Wu S, Li H, Yang H, Zhang X, Li Z, Xu S: Quantitative analysis on collagen morphology in aging skin based on multiphoton microscopy, J Biomed Opt 2011, 16:040502

58. Park JH, Kim SR, An HJ, Kim WJ, Choe M, Han JA: Esculetin promotes type I procollagen expression in human dermal fibroblasts through MAPK and PI3K/Akt pathways, Mol Cell Biochem 2012, 368:61-67

59. Ono I, Akasaka Y, Kikuchi R, Sakemoto A, Kamiya T, Yamashita T, Jimbow K: Basic fibroblast growth factor reduces scar formation in acute incisional wounds, Wound Repair Regen 2007, 15:617-623

60. Kleindorp R, Flachsbart F, Puca AA, Malovini A, Schreiber S, Nebel A: Candidate gene study of FOXO1, FOXO4, and FOXO6 reveals no association with human longevity in Germans, Aging Cell 2011, 10:622-628

61. Li Y, Wang WJ, Cao H, Lu J, Wu C, Hu FY, Guo J, Zhao L, Yang F, Zhang YX, Li W, Zheng GY, Cui H, Chen X, Zhu Z, He H, Dong B, Mo X, Zeng Y, Tian XL: Genetic association of FOXO1A and FOXO3A with longevity trait in Han Chinese populations, Hum Mol Genet 2009, 18:4897-4904

62. Poindexter NJ, Williams RR, Powis G, Jen E, Caudle AS, Chada S, Grimm EA: IL-24 is expressed during wound repair and inhibits TGFalpha-induced migration and proliferation of keratinocytes, Exp Dermatol 2010, 19:714-722

63. Gregorio J, Meller S, Conrad C, Di Nardo A, Homey B, Lauerma A, Arai N, Gallo RL, Digiovanni J, Gilliet M: Plasmacytoid dendritic cells sense skin injury and

promote wound healing through type I interferons, J Exp Med 2010, 207:2921-2930

64. Gardner H, Broberg A, Pozzi A, Laato M, Heino J: Absence of integrin alpha1beta1 in the mouse causes loss of feedback regulation of collagen synthesis in normal and wounded dermis, J Cell Sci 1999, 112 (Pt 3):263-272

65. Ekstrand AJ, Cao R, Bjorndahl M, Nystrom S, Jonsson-Rylander AC, Hassani H, Hallberg B, Nordlander M, Cao Y: Deletion of neuropeptide Y (NPY) 2 receptor in mice results in blockage of NPY-induced angiogenesis and delayed wound healing, Proc Natl Acad Sci U S A 2003, 100:6033-6038

66. Akita S, Daian T, Ishihara H, Fujii T, Akino K: Leukemia inhibitory factor-transfected embryonic fibroblasts and vascular endothelial growth factor successfully improve the skin substitute wound healing by increasing angiogenesis and matrix production, J Dermatol Sci 2004, 36:11-23

67. Meyer M, Muller AK, Yang J, Moik D, Ponzio G, Ornitz DM, Grose R, Werner S: FGF receptors 1 and 2 are key regulators of keratinocyte migration in vitro and in wounded skin, J Cell Sci 2012,

68. Sun LL, Xu LL, Nielsen TB, Rhee P, Burris D: Cyclopentyladenosine improves cell proliferation, wound healing, and hair growth, J Surg Res 1999, 87:14-24

Figure legends

Figure 1. Skin wound healing is accelerated in *Foxo1*$^{+/-}$ mice.

(A) Gene expression of murine Foxo family in skin wound healing measured by qPCR relative to 18S ribosomal RNA (n = 4-6). (B) Representative images for gross appearances of excisional wound in WT and *Foxo1*$^{+/-}$ mice (C) The proportion of the wound remaining open relative to the initial wound area at each time point (n = 12). (D) IHC for FOXO1 and neutrophils showing neutrophils, epithelium and hair follicle expressing FOXO1 1 d after injury in WT mice. Nuclei were counter stained with DAPI (wound margin [closed arrowhead], leading edge of epithelia [arrow], and FOXO1-expressing neutrophils [open arrowheads]). (E and F) IHC of FOXO1 and F4/80 or CD31 showing wound-infiltrated macrophages (E), fibroblasts (E, arrowhead), and endothelial cells (F) at 7 d after injury in WT mice. (G) H&E staining of re-epithelialization (wound margin [arrowheads] and the leading edge of epithelia [arrows]). Upper panels correspond to the higher-power field of the lower panels. (H) Measurement of epithelial tongue on 3 d after injury (n = 13). (I) Middle of wound tissue at 14 d after injury stained with Masson's Trichrome, and the extent (cross-sectional area) of granulation tissue visualized and quantified at the mid-point of the wound (indicated by dotted line) (wound margin [arrowheads]). (J) Quantification of the area of granulation tissue 14 d after injury (n = 6). Scale bars = 10 μm (E and F), 100 μm (D and lower panels in G), 500 μm (low-power fields in G and I). All values represent mean ± SEM. *P < 0.05, **P < 0.01, ***P < 0.001.

Figure 2. Attenuation of neutrophil and macrophage infiltration and inflammatory responses at wound sites of *Foxo1*$^{+/-}$ mice.

(A) IHC for neutrophils (red) showing the number of wound-infiltrated neutrophils at wound sites 1 d after injury, which is reduced in *Foxo1*$^{+/-}$ mice compared with WT mice (nuclei were counter stained with DAPI). (B) MPO concentration using ELISA reveals that MPO levels at wound sites of *Foxo1*$^{+/-}$ mice are significantly reduced compared with WT mice (n = 8 per group). (C) IHC for macrophages using F4/80 at the middle area of wound sites 7 d after injury. (D) Quantification of F4/80-positive macrophages at wound sites of WT mice (n = 6 per group for 3 d and n = 5 per group for 7 d) and *Foxo1*$^{+/-}$ mice (n = 6 per group for 3 and 7 d). (E) Western immunoblot of pNF-κB p65 and total NF-κB. Full scans for western immunoblot in Supplemental Figure S5A. (F) Densitometric analysis for pNF-κB activity over total NF-κB (n = 4-5). Scale bars = 10 μm (A and C). All values represent mean ± SEM. *P < 0.05.

Figure 3. ERK1/2 activation and Myosin IIb expression is enhanced at wound sites of *Foxo1*$^{+/-}$ mice.

(A) FOXO1 binding activity in the nuclear wound tissue extract was measured by immobilized oligonucleotide ELISA. FOXO1 consensus oligonucleotide-treated extracts were used as negative control (n = 2-4). (B) Western immunoblot of wound tissue at 3 d shows weak expression of total FOXO1 and pFOXO1 (Thr24) at wound sites of *Foxo1*$^{+/-}$ mice. Bands for total FOXO3A, pFOXO3A (Ser318/321), and FOXO4 remain unchanged in both groups. Full scans for western immunoblot in Supplemental

Figure S5B. (C) Western immunoblot of pERK1/2 (Thr202/Tyr204), total ERK1/2, pAKT (Ser473), total AKT, and Myosin IIb. Full scans for western immunoblot in Supplemental Figure S5C. (D) Densitometric analysis of pERK1/2 (Thr202/Tyr204) and pAKT (Ser473) over total ERK1/2 and AKT, respectively, and Myosin IIb (n = 4-5). (E) Wound scratch assay 24 h after treatment of mFGF2 in PKs with control (left) or Foxo1 siRNAs (right). (F) Wound closure ratio (n = 4). (G) Confocal images of pERK in mFGF2-treated control PKs (left) and Foxo1 siRNA-treated PKs (right) 24 h after scratching (n = 3). (H) Fluorescence intensity of pERK by mFGF2 24 h after scratching in control PKs and Foxo1 siRNA-treated PKs (n = 3). Scale bar = 100 μm (E), and 50 μm (G). All values represent mean ± SEM. *P < 0.05.

Figure 4. Scarring at wound sites is attenuated in *Foxo1*$^{+/-}$ mice.

(A) Gross appearance of scarring at the incisional wound 21 d after injury (*wound edge). Images shown are representative of six independent experiments. (B) Picrosirius red-stained sections of incisional wound sites at 21 d after injury for analysis of collagen fibers and alignments (type I collagen [red and yellow]; type III collagen [green]; wound edge [arrowhead]). Granulation tissue was visualized at the mid-point of the wound (indicated by dotted line). Images shown are representative of eight independent experiments. Low magnifications were taken as non-polarized images. High-magnification details from boxed areas indicated are differential interference contract images using polarized light microscopy. (C) TEM images of connective tissue from mid-wound sites 21 d after injury. High magnification insets illustrate differing

collagen fibril diameters in this tissue. (D) Histogram of total range of fibril diameters in the wound site 21 d after injury (n = 1090 fibrils from 3 WT mice and n = 1354 fibrils from 3 *Foxo1*$^{+/-}$ mice). Fibril diameters at wound sites of *Foxo1*$^{+/-}$ mice tend to be smaller than WT mice. (E) Quantification of vacant extracellular spaces in wound sites at 21 d (n = 3-4). (F) Quantification of gene expression of Col1α1 7 d after injury at wound sites (measured by qPCR), relative to 18S ribosomal RNA (n = 8). Scale bars = 50 μm (B), and 1 μm and 100 nm (inset box) (C). All values represent mean ± SEM. *P < 0.05.

Figure 5. Skin wound healing is accelerated in Foxo1 AS ODN-treated wounds. (A) Optimization of Foxo1 AS ODNs *in vitro*. Cleavage was visualized when transcribed Foxo1 mRNA was incubated with control and AS ODNs *in vitro* (representative of n = 2 independent experiments) (M1 and M2 = RNA loading marker). Sequences are shown in Table 2. Foxo1 AS ODN (1717) is more efficient than other Foxo1 AS ODNs. (B) Western immunoblot from wound sites (6 h after injury) to detect the effective dose of Foxo1 AS ODN (1717) to decrease FOXO1 protein expression in wounds *in vivo*. Full scans for western immunoblot in Supplemental Figure S5D. (C) Quantification of FOXO1 protein expression in wound sites exposed to 10 μM Foxo1 AS ODN (1717) (n = 6 per group) reveals that FOXO1 is significantly reduced. Data are presented as the mean ± SEM and analyzed by Tukey's multiple comparison tests. (D) Representative photomicrographs for gross appearances of excisional control and Foxo1 AS ODN-treated wounds at various time points after wounding (n = 12). (E) The

proportion of the wound remaining open relative to the initial wound area at each time point after the injury in control versus Foxo1 AS ODN-treated wounds (n = 12 per group). All values represent mean ± SEM. *P < 0.05, **P < 0.01.

Figure 6. Expression of FOXO1 at human keloids.

(A to C) IHC for FOXO1 shows that FOXO1 (brown) is highly present in basal lamina keratinocytes at human keloid sites in the Japanese population (nuclei are stained with hematoxylin [violet]) (FOXO1 expressing cells [arrowheads]). (D and E) FOXO1 is present in normal epidermis and dermis in the immediate vicinity of keloid sites compared with mature keloid sites. (F) IHC for FOXO1 shows highly prominent FOXO1-positive cells at the surface and deep in keloid sites of African Americans compared with Japanese (mature deep keloid sites are shown inset). Micrographs are representative of 3 and 6 sections for D to F and A to C, respectively. (G) Percentage of FOXO1-positive cells at the intact skin in the immediate vicinity of keloid sites (3 case) and keloid sites (6 case). (H) Percentage of FOXO1-positive cells at mature keloid sites of an African American (3 case) and two Japanese (6 case) patients. (I) A proposed model of the exacerbation of keloids by FOXO1. Elevated expression of FOXO1 at the epidermis may cause hyperplasia of keloids. In contrast, numbers of FOXO1-expressing cells at deeply mature keloid sites are markedly reduced. Intact skin in the vicinity of keloids appears normal. However, expression of FOXO1 is markedly increased compared with mature keloid, suggesting that FOXO1 positive cells are associated with keloid expansion. Collectively, many FOXO1-expressing cells produce collagen and

enhance the inflammatory response, leading to the exacerbation of keloid scarring. Scale bars = 500 μm (A and D), and 100 μm (B, C, E, and F). All values represent mean ± SEM. *P < 0.05.

Table 1. **List of antibodies**

Primary Ab #	**Species**	**Dilution**	**Blocking †**	**Secondary Ab ***	**Dilution**
AKT (pan) (CST)	Rabbit	1:1000 (WB)	PVDF Blocking Reagent (TOYOBO)	α-rabbit IgG HRP-linked Whole Antibody (GE Healthcare)	1:10000
Phosho-AKT (pan) (CST)	Rabbit	1:1000 (WB)	PVDF Blocking Reagent (TOYOBO)	α-rabbit IgG HRP-linked Whole Antibody (GE Healthcare)	1:10000
CD31 (BD Pharmingen)	Rat	1:200 (IHC-f)	Blocking One Histo (Nacalai Tesque)	Goat α-rabbit IgG Alexa Fluor 568 (Molecular Probes)	1:400
F4/80 (Abcam)	Rat	1:400 (IHC-p)	Blocking One Histo (Nacalai Tesque)	Goat α-rabbit IgG Alexa Fluor 568 (Molecular Probes)	1:800
FOXO1 (Abcam)	Rabbit	1:400 (IHC-p)	Blocking One Histo (Nacalai Tesque)	Goat α-rabbit IgG Alexa Fluor 488 or 568 (Molecular Probes)	1:800 1:200

				Biotinylated α-rabbit IgG (Vector lab)	
FOXO1 (CST)	Rabbit	1:1000 (WB)	PVDF Blocking Reagent (TOYOBO)	α-rabbit IgG HRP-linked Whole Antibody (GE Healthcare)	1:10000
Phosho-FOXO1 (Thr24) (CST)	Rabbit	1:1000 (WB)	PVDF Blocking Reagent (TOYOBO)	α-rabbit IgG HRP-linked Whole Antibody (GE Healthcare)	1:10000
FOXO3A (CST)	Rabbit	1:1000 (WB)	PVDF Blocking Reagent (TOYOBO)	α-rabbit IgG HRP-linked Whole Antibody (GE Healthcare)	1:10000
Phosho-FOXO3A (Ser318/321) (CST)	Rabbit	1:1000 (WB)	PVDF Blocking Reagent (TOYOBO)	α-rabbit IgG HRP-linked Whole Antibody (GE Healthcare)	1:10000
FOXO4 (CST)	Rabbit	1:1000 (WB)	PVDF Blocking Reagent	α-rabbit IgG HRP-linked Whole	1:10000

			(TOYOBO)	Antibody (GE Healthcare)	
p44/42 MAPK (ERK1/2) (CST)	Rabbit	1:1000 (WB)	PVDF Blocking Reagent (TOYOBO)	α-rabbit IgG HRP-linked Whole Antibody (GE Healthcare)	1:10000
Phosho-p44/42 MAPK (ERK1/2) (CST)	Rabbit	1:1000 (WB) 1:200 (ICC)	PVDF Blocking Reagent (TOYOBO) Blocking One Histo (Nacalai tesque)	α-rabbit IgG HRP-linked Whole Antibody (GE Healthcare) Goat α-rabbit IgG Alexa Fluor 568 (Molecular Probes)	1:10000 1:1000
PCNA (abcam)	mouse	1:400 (IHC-p and -f)	Blocking One Histo (Nacalai tesque)	Histofine mousestain kit (Nichirei biosciences Inc)	
Myosin IIb (CST)	Rabbit	1:1000 (WB)	PVDF Blocking Reagent (TOYOBO)	α-rabbit IgG HRP-linked Whole Antibody	1:10000

				(GE Healthcare)	
NF-κB p65 (CST)	Rabbit	1:1000 (WB)	PVDF Blocking Reagent (TOYOBO)	α-rabbit IgG HRP-linked Whole Antibody (GE Healthcare)	1:10000
Phospho-NF-κB p65 (Ser536) (CST)	Rabbit	1:1000 (WB)	PVDF Blocking Reagent (TOYOBO)	α-rabbit IgG HRP-linked Whole Antibody (GE Healthcare)	1:10000
Neutrophil (Abcam)	Rat	1:400 (IHC-p)	Blocking One Histo (Nacalai Tesque)	Goat α-rabbit IgG Alexa Fluor 488 (Molecular Probes)	1:800
α-tubulin (Abcam)	Rabbit	1:1000 (WB)	PVDF Blocking Reagent (TOYOBO)	α-rabbit IgG HRP-linked Whole Antibody (GE Healthcare)	1:10000
β-actin (Abcam)	Rabbit	1:5000 (WB)	PVDF Blocking Reagent (TOYOBO)	α-rabbit IgG HRP-linked Whole Antibody (GE Healthcare)	1:10000

Abbreviations: CST, Cell Signaling Technology; f, frozen section; ICC,

immunocytochemistry; p, paraffin section; WB, western immunoblotting.

***** Overnight incubation at 4°C (IHC-p, HIC-f, ICC and WB).

† Blocking time: 2 h at room temperature.

‡ Incubation for 1 h at room temperature.

Table 2. Sequences for control and AS ODNs

Name	Sequence (5’-3’)
Control ODN	5’-GTGTAACACGTCTATACG-3’
Foxo1 AS (1273)	5’-CTGGAGAGATGCTTTTTT-3’
Foxo1 AS (1341)	5’-GACCCAGGACTCGCAGGC-3’
Foxo1 AS (1686)	5’-GAATTTAGACTGGTGTTT-3’
Foxo1 AS (1692)	5’-CTGGGTGAATTTAGACTG-3’
Foxo1 AS (1717)	5’-GTATGTGTACTTTGAGTA-3’
Foxo1 AS (1914)	5’-AGGACCCGACTGTTGGGT-3’
Foxo1 AS (1986)	5’-ATTTTGTTATGAGATGCC-3’
Foxo1 AS (2070)	5’-TTCACCACATGGGGCAGG-3’
Foxo1 AS (2095)	5’-CATGGCAGATGTGTGAGG-3’
Foxo1 AS (2138)	5’-ACAGAGGCACTTGTAAAG-3’
Foxo1 AS (2208)	5’-ATCCTACCATAGCCATTG-3’

Table 3. Expression of skin wound-related genes

Gene symbol: name	Ratio	Molecular Function	Reference
Il24: interleukin 24	2.478	Cytokine	62
Ifna1/Ifna13: interferon, alpha 1	2.199	Cytokine	63
Itga1: integrin, alpha 1	2.316	Receptor	64
Notch1	1.944	Receptor	34
Adipoq: adiponectin, C1Q and collagen domain containing	1.824	Cytokine	8, 9
Npy2r: neuropeptide Y receptor Y2	1.821	Receptor	65
Lif: leukemia inhibitory factor	1.777	Cytokine	66
Fgf2: fibroblast growth factor 2 (basic)	1.647	Growth factor	32, 33, 67
Myh10: myosin, heavy chain 10, non-muscle	1.641	Actin-based motor protein	51
Adora1: adenosine A1 receptor	1.637	Receptor	68
Foxo1: forkhead box O1	−1.92	Transcription factor	

Table 3. Gene expressions from the microarray data set (Supplementary Table S2). Compared with WT mice, a ratio > 1.5 in *Foxo1*$^{+/-}$ mice indicates a significant up-regulation (n = 3 per group). *Il24* may be a negative regulator of skin wound healing. Expression of *Foxo1* serves as a positive control.

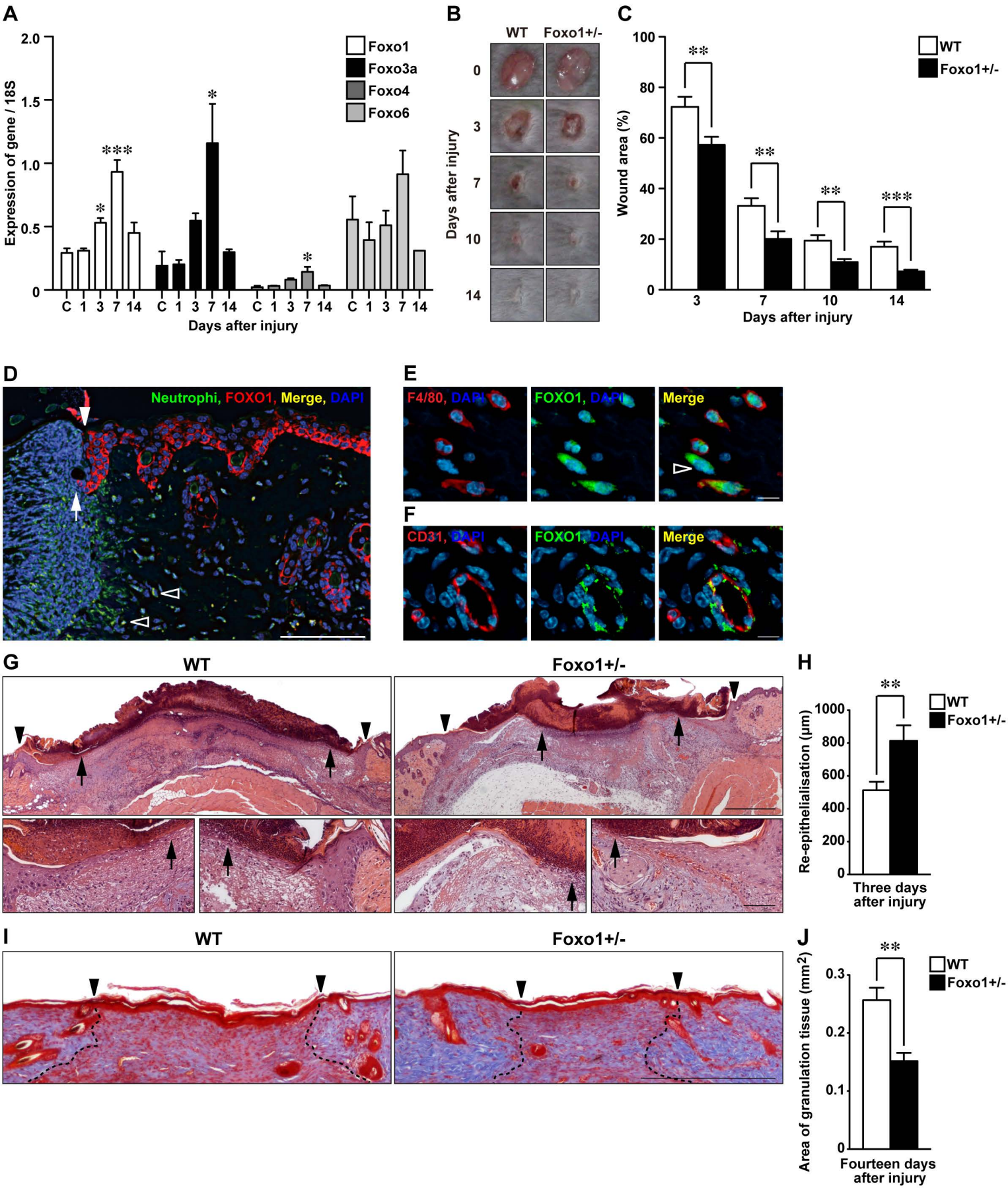
A
Expression of gene / 18S
Foxo1
Foxo3a
Foxo4
Foxo6
Days after injury
B
WT
Foxo1+/-
Days after injury
C
Wound area (%)
WT
Foxo1+/-
Days after injury
D
Neutrophi, FOXO1, Merge, DAPI
E
F4/80, DAPI
FOXO1, DAPI
Merge
F
CD31, DAPI
FOXO1, DAPI
Merge
G
WT
Foxo1+/-
H
Re-epithelialisation (μm)
WT
Foxo1+/-
Three days after injury
I
WT
Foxo1+/-
J
Area of granulation tissue (mm2)
WT
Foxo1+/-
Fourteen days after injury

Figure 1

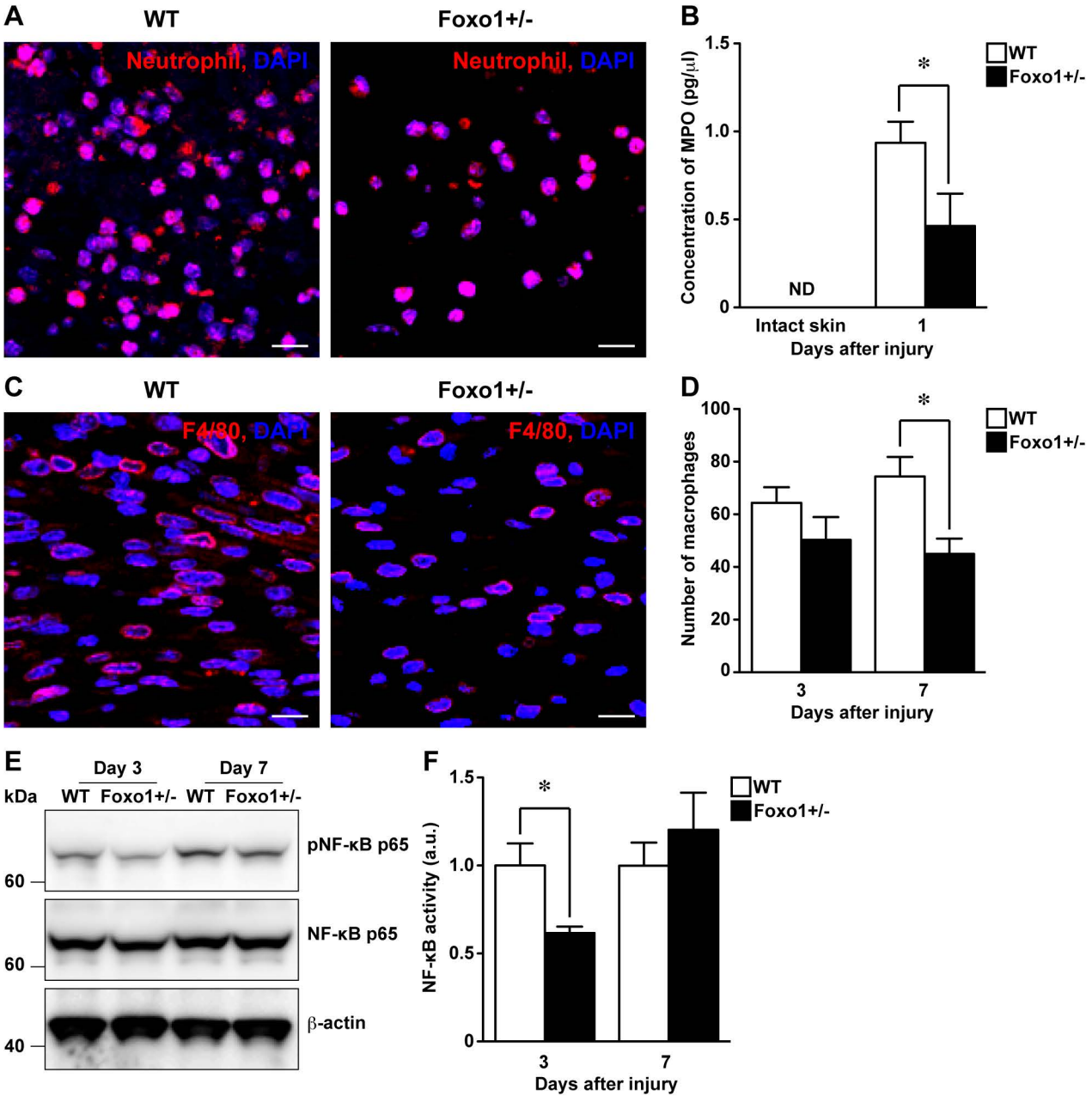
A
WT
Foxo1+/-
Neutrophil, DAPI
Neutrophil, DAPI
B
Concentration of MPO (pg/μl)
1.5
1.0
0.5
0
*
WT
Foxo1+/-
ND
Intact skin
1
Days after injury
C
WT
Foxo1+/-
F4/80, DAPI
F4/80, DAPI
D
Number of macrophages
100
80
60
40
20
0
*
WT
Foxo1+/-
3
7
Days after injury
E
Day 3
Day 7
kDa
WT
Foxo1+/-
WT
Foxo1+/-
60
pNF-κB p65
60
NF-κB p65
40
β-actin
F
NF-κB activity (a.u.)
1.5
1.0
0.5
0
*
WT
Foxo1+/-
3
7
Days after injury

Figure 2

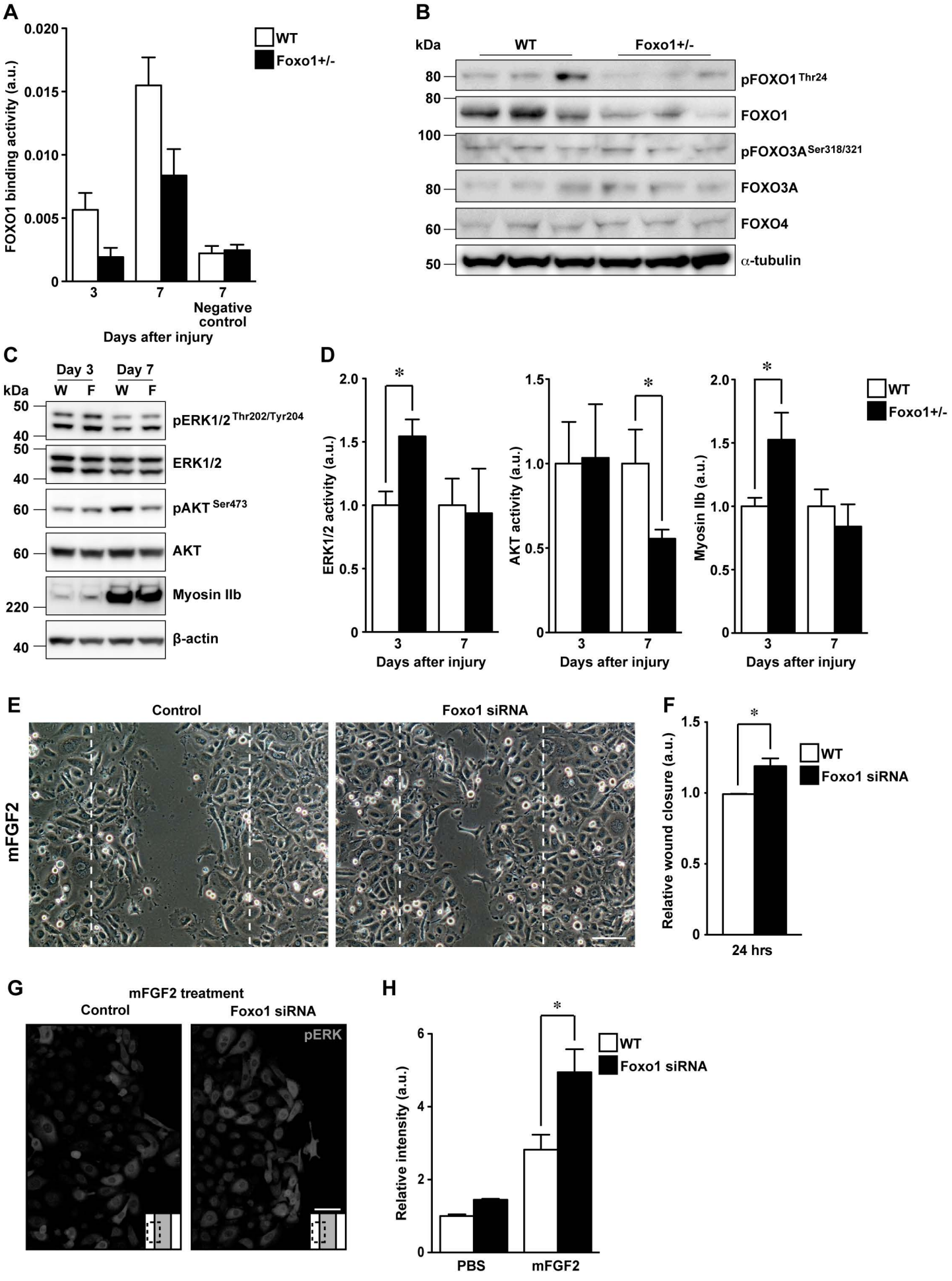
A
FOXO1 binding activity (a.u.)
0.020
0.015
0.010
0.005
0
WT
Foxo1+/-
3
7
7
Negative control
Days after injury
B
kDa
WT
Foxo1+/-
80
pFOXO1 Thr24
80
FOXO1
100
pFOXO3A Ser318/321
80
FOXO3A
60
FOXO4
50
α-tubulin
C
Day 3
Day 7
kDa
W F W F
50
pERK1/2 Thr202/Tyr204
40
50
ERK1/2
40
60
pAKT Ser473
60
AKT
220
Myosin IIb
40
β-actin
D
ERK1/2 activity (a.u.)
AKT activity (a.u.)
Myosin IIb (a.u.)
2.0
1.5
1.0
0.5
0
*
3
7
Days after injury
WT
Foxo1+/-
E
Control
Foxo1 siRNA
mFGF2
F
Relative wound closure (a.u.)
1.5
1.0
0.5
0
*
WT
Foxo1 siRNA
24 hrs
G
mFGF2 treatment
Control
Foxo1 siRNA
pERK
H
Relative intensity (a.u.)
6
4
2
0
*
WT
Foxo1 siRNA
PBS
mFGF2

Figure 3

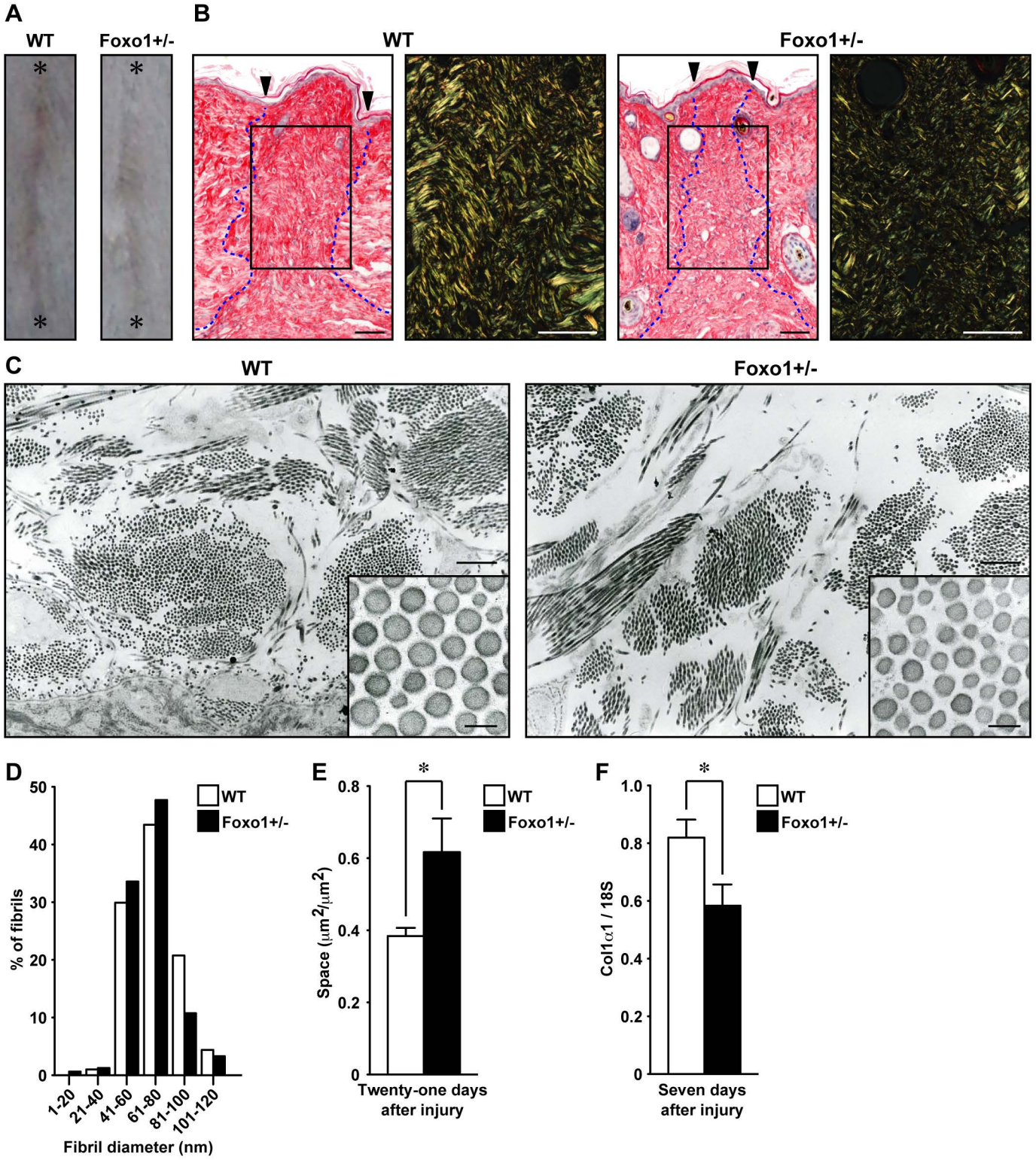
A
WT
Foxo1+/-
B
WT
Foxo1+/-
C
WT
Foxo1+/-
D
WT
Foxo1+/-
% of fibrils
50
40
30
20
10
0
1-20
21-40
41-60
61-80
81-100
101-120
Fibril diameter (nm)
E
*
WT
Foxo1+/-
Space (μm2/μm2)
0.8
0.6
0.4
0.2
0
Twenty-one days
after injury
F
*
WT
Foxo1+/-
Col1α1 / 18S
1.0
0.8
0.6
0.4
0.2
0
Seven days
after injury

Figure 4

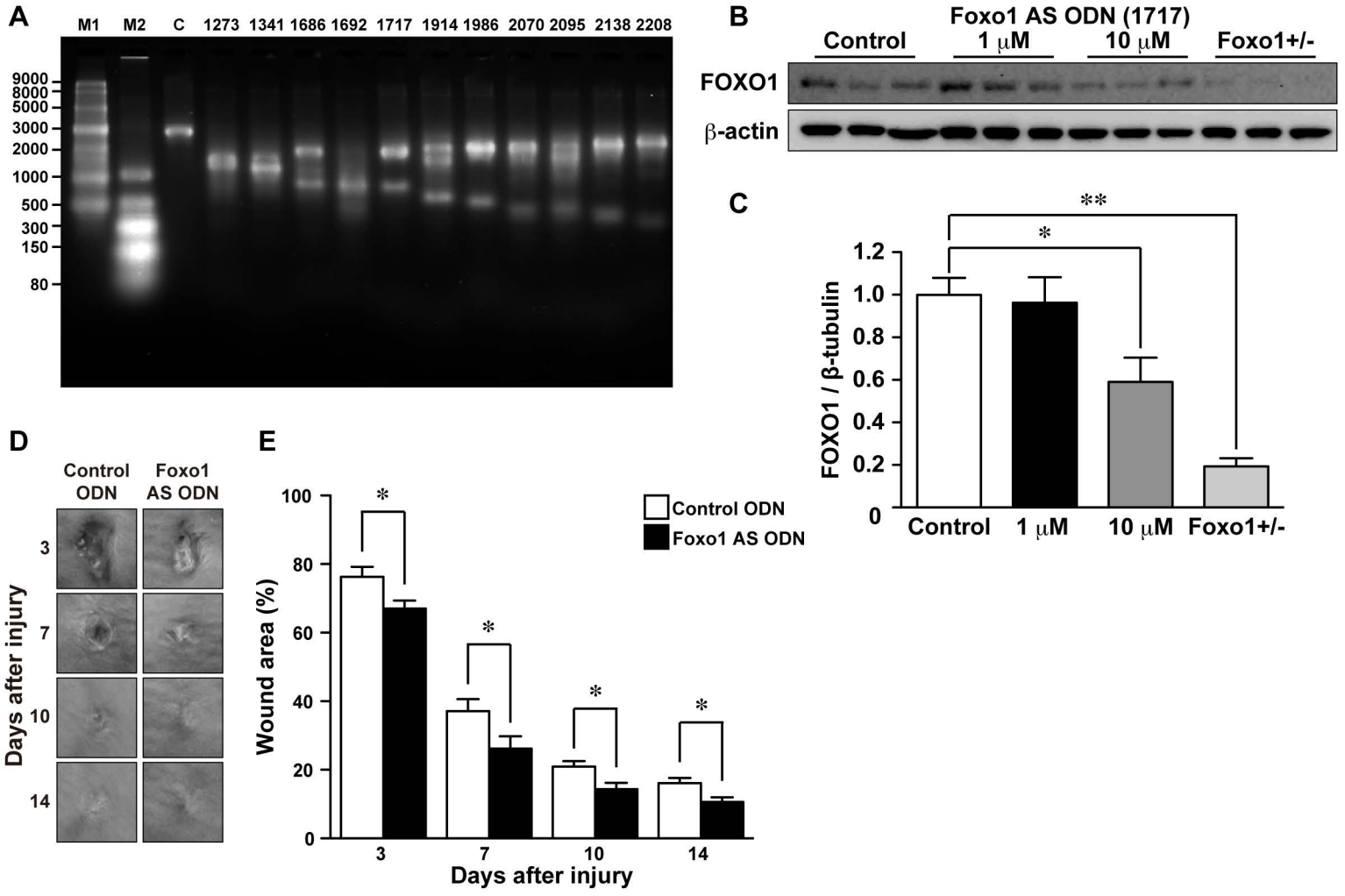
A
M1
M2
C
1273
1341
1686
1692
1717
1914
1986
2070
2095
2138
2208
9000
8000
5000
3000
2000
1000
500
300
150
80
B
Foxo1 AS ODN (1717)
Control
1 μM
10 μM
Foxo1+/-
FOXO1
β-actin
C
**
*
FOXO1 / β-tubulin
1.2
1.0
0.8
0.6
0.4
0.2
0
Control
1 μM
10 μM
Foxo1+/-
D
Control ODN
Foxo1 AS ODN
Days after injury
3
7
10
14
E
Control ODN
Foxo1 AS ODN
Wound area (%)
100
80
60
40
20
0
*
3
7
10
14
Days after injury

Figure 5

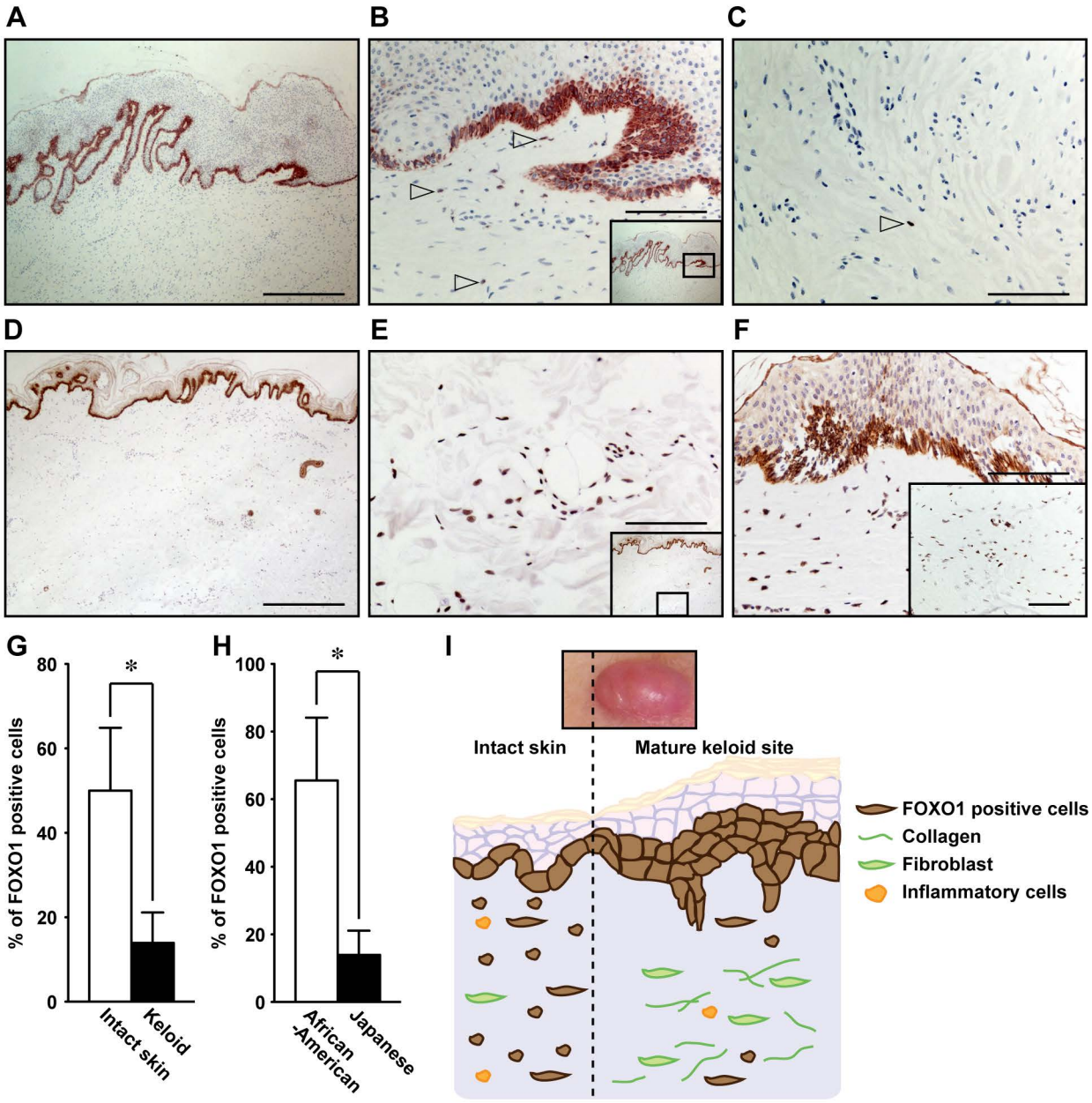
A
B
C
D
E
F
G
% of FOXO1 positive cells
80
60
40
20
0
*
Intact skin
Keloid
H
% of FOXO1 positive cells
100
80
60
40
20
0
*
African -American
Japanese
I
Intact skin
Mature keloid site
FOXO1 positive cells
Collagen
Fibroblast
Inflammatory cells

Figure 6